Age of Information Outage Probability Analysis for Computation Offloading in IIoT Networks

Tan Zheng Hui Ernest, and A S Madhukumar,

***Abstract*—In this paper, the performance characterization of outage probability and age of information (AoI) for computation offloading in multi-access edge computing (MEC)-enabled industrial Internet-of-Things (IIoT) networks is investigated. Through newly obtained cumulative density functions of signal-to-interference-plus-noise ratios in the MEC-enabled IIoT network, closed-form AoI outage probability expressions are derived for MEC-based computation offloading (MEC-CO) and cloud-only computation offloading (CLD-CO) protocols assuming Rician fading, base station locations modeled as binomial point processes, and Gamma distributed delays in the wired backhaul. Suitable communication radius and task sizes to enable reliable computation offloading in both rural and urban IIoT scenarios are identified for both MEC-CO and CLD-CO through extensive analysis, where it is shown that MEC-CO attains superior AoI performance over CLD-CO.**

***Index Terms*—Multi-Access Edge Computing, Computation Offloading, Industrial, Internet-of-Things, Age of Information.**

I. Introduction

Recent advances in wireless technologies has led to increased interest in industrial Internet-of-Things (IIoT) networks for future smart factory applications in industry and academia [1]–[3]. The interest is mainly due to the fact that existing factories and industrial buildings have limited connectivity and are inadequate in supporting IIoT use cases, e.g., autonomous mobile robots (AMRs) and actuators, requiring flexible connectivity, low deployment and maintenance costs, ultra-reliable low-latency communications, and heavy computations [1]–[6].

In addressing the above challenges, multi-access edge computing (MEC)-enabled computation offloading has been widely investigated as a potential solution to support future smart factory applications in IIoT networks [6]. In such MEC-enabled IIoT networks, tasks are either offloaded to a small cell base station (SBS) equipped with an MEC server, or to a remotely cloud server, for computation depending on the experienced latency [5], [7]. For instance, a joint communication and computation offloading strategy was proposed for a hierarchical IIoT network in [5]. Specifically, the authors show that end-to-end latency experienced by IIoT devices can be minimized by jointly considering offloading decisions, server processing rates, and IIoT device association. In [6], the authors proposed a stochastic computation offloading framework that adaptively offloads tasks between MEC and cloud servers in MEC-enabled IIoT networks based on prevailing traffic conditions. Similarly in [8], the authors proposed a cost-efficient computation offloading strategy that adaptively offload tasks between IIoT devices and servers in IIoT networks.

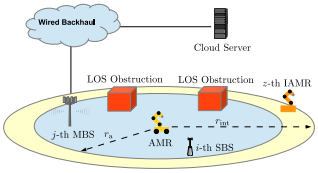

Fig. 1. An illustration of the AMR in the MEC-enabled IIoT network.

Despite extensive studies, there still remains limited work on the characterization of outage probability and the age of information (AoI), which measures the freshness of information, of computation offloading in MEC-enabled IIoT networks [9]. Existing studies on computation offloading in MEC-enabled IIoT networks have also mainly investigated latency or energy usage minimization, e.g., [5], [6], [8]. While there exist studies on the performance charaterization of computation offloading for cellular networks, e.g., [7], the relevance to MEC-enabled IIoT networks is limited due to harsh IIoT environments, line-of-sight (LOS) blockage, and interference from other IIoT devices. Specifically, closed-form AoI outage probability expressions which account for the above factors in IIoT networks are, to the best of the authors knowledge, unavailable in the literature.

Therefore, in this paper, new closed-form expressions are obtained for the cumulative density function (CDF) of signal-to-interference-plus-noise ratios (SINRs) in the MEC-enabled IIoT network. Through the new CDF expressions, closed-form AoI outage probability expressions are obtained for MEC-based computation offloading (MEC-CO) and cloud-only computation offloading (CLD-CO) protocols. Extensive analysis in both urban micro (UMi) and rural macro (RMa) scenarios show the MEC-CO protocol achieving lower AoI outage probability than the CLD-CO protocol. The choice of communication radius and task size for reliable computation offloading in both UMi and RMa scenarios are also identified through AoI outage probability analysis. The remainder of this paper is organized as follows. The proposed system model is introduced in Section II, with closed-form AoI outage probability expressions derived Section III. Finally, the results of the numerical results are presented in Section IV before the conclusion of the paper in Section V.

II. System Model

A two-tiered heterogeneous MEC-enabled IIoT network comprising an AMR without local computing capability [1],

Tan Zheng Hui Ernest is with the Advanced Remanufacturing and Technology Centre, Agency for Science, Technology and Research, Singapore e-mail: (ernest_tan@artc.a-star.edu.sg).

A S Madhukumar is with the School of Computer Science and Engineering, Nanyang Technological University, Singapore e-mail: (asmadhukumar@ntu.edu.sg).

M_{SBS} SBSs equipped with MEC servers in the first tier, and M_{MBS} macro base stations (MBSs) in the second tier, is shown in Fig. 1. The AMR is assumed to have tasks which are offloaded in packets of K_{size} bits to SBSs via cellular uplink transmissions for computation, i.e., MEC-CO protocol. [1] [2] Tasks are also offloaded to a cloud server located $N \geq 3$ hops from the AMR via MBSs over cellular uplink transmissions and $N-1$ wired backhaul links, when computation offloading to SBSs is in outage, i.e., CLD-CO protocol. [3] Furthermore, Rician fading, imperfect channel state information (CSI), interference, and LOS blockage, are assumed in this work due to reflecting objects in IIoT environments [4], AMR mobility, presence of M_{int} interfering AMRs (IAMRs), and LOS obstructions from metallic objects [2], respectively. [4] [5] Finally, it is assumed that the AMR associates to SBSs and MBSs with the strongest instantaneous SINRs.

A. Received SINR and Wired Backhaul Models

Let the AMR be centered at an origin O. Then, the spatial locations of the SBSs and MBSs are assumed to be uniformly distributed around a disc centered at O with a communications radius r_{a} and angle $[0, 2\pi)$. Similarly, the spatial locations of the IAMRs are assumed to be uniformly distributed around an annulus centered at O with minimum radius r_{a}, maximum radius r_{int}, and angle $[0, 2\pi)$. [6] Let d_i, d_j, and d_z, denote the Euclidean distance to the i-th SBS, j-th MBS, and z-th IAMRs, respectively, from the AMR. Then, the probability density function (PDF) $f_{d_x}(w)$ of $d_x, x \in \{i, j\}$ is given as $f_{d_x}(w) = \frac{2w}{r_{\text{a}}^2}, 0 \leq w \leq r_{\text{a}}$ [11], while the PDF of $f_{d_z}(w)$ of d_z is given as $f_{d_z}(w) = \frac{2w}{r_{\text{int}}^2 - r_{\text{a}}^2}, 0 \leq r_{\text{a}} \leq w < r_{\text{int}}$ [12]. Based on the imperfect CSI model in [10], let $h_x = \epsilon \hat{h}_x + \sqrt{1-\epsilon^2} e_x, x \in \{i, j\}$ be the channel gain between node-x and the AMR, $\hat{h}_x$ be the estimated channel gain, and e_x be the estimation error, where $\epsilon = J_0(2\pi f_d T)$ is the correlation coefficient, $0 \leq \epsilon < 1$, $J_0(\bullet)$ is the zero-order Bessel function of the first kind [13, eq. (9.1.10)], T is the feedback period, $f_d = \frac{v f_c}{c}$ is the maximum Doppler frequency, f_c is the carrier frequency, v is the speed of the AMR in m/s, and $c = 3 \times 10^8$ m/s. Let $|\hat{h}_x|^2$ be modeled as a non-centered Chi-squared distributed random variable (RV) with average received power $\Omega_x = \bar{P}_t \epsilon^2, x \in \{i, j\}$ and Rician factor K_x, where $\bar{P}_t = P_t / (L_0 \eta)$ is the normalized transmit power, P_t is the transmit power, L_0 is the pathloss, $\eta = -174 + 10 \log_{10}(B_W)$ is the noise power in dBm, and B_W is the bandwidth. Similarly, let $|e_x|^2, x \in \{i, j\}$ be modeled as an exponentially distributed RV with average received power $\mu_x = \bar{P}_t (1 - \epsilon^2)$ and $|h_z|^2$ be modeled as a non-centered Chi-squared distributed RV with average received power $\Omega_z = \bar{P}_t$ and Rician factor K_z, where h_z is the channel gain between the z-th IAMR and the associated base station.

Then, the received instantaneous SINR at the i-th SBS (γ_i) or j-th MBS (γ_j) is modeled as:

$$\gamma_x = \frac{\beta_x |\hat{h}_x|^2 d_x^{-l}}{1 + |e_x|^2 d_x^{-l} + \sum_{z=1}^{M_{\text{int}}} |h_z|^2 d_z^{-l}}, \tag{1}$$

where $x \in \{i, j\}$, l is the pathloss exponent, and β_x is the LOS occurrence. Specifically, β_x is modeled as a Bernoulli RV where $\beta_x = 0$ denotes non LOS (NLOS) with probability $1 - \mathbb{P}_{\text{LOS}}$, and $\beta_x = 1$ indicates LOS with probability $\mathbb{P}_{\text{LOS}}$ [14]. In this way, NLOS occurrence due to obstruction from walls and metallic objects, e.g., other AMRs, can be accounted for in the IIoT network [2], where instantaneous SINR can be close to zero [15]. It is also worth noting that imperfect CSI and the M_{int} IAMRs are the main sources of interference in the considered MEC-enabled IIoT network, which is modeled in (1) through $|e_x|^2$ and $|h_z|^2$, respectively.

Separately, for the $N-1$ wired backhaul links, the delay of the b-th wired backhaul link $T_b, 1 \leq b \leq N-1$ is modeled as a Gamma distributed RV [16] with shaping parameter $m_\omega = d_b$ and scale parameter $\theta_\omega = c_{\text{wired}} K_{\text{size}}$. The average delay of the b-th wired backhaul link (ω) is then given as $\omega = \theta_\omega m_\omega$, where $d_b \geq r_{\text{a}}$ and c_{wired} respectively accounts for the length the b-th wired backhaul link and the propagation delay (seconds) per bit and unit backhaul length.

B. AoI Model

At the i-th SBS, j-th MBS, b-th wired backhaul link, and the cloud server, older packets are dropped as the reception of new packets is assumed to render older tasks obsolete. Furthermore, for the j-th MBS and the b-th wired backhaul link, packets are either retransmitted until successful reception at the next hop, or dropped in favor of newer tasks since older packets are assumed to be obsolete [9]. Similar to [9], the AoI in the MEC-enabled IIoT network is assumed to evolve in discrete time steps of t. As such, AoI is evaluated once at the end of time step t for each of the N hops, i.e., at the SBSs, MBSs, b-th wired backhaul link, and cloud server. [7]

Let $\Delta_x[t], x \in \{i, j, b, \text{CS}\}$ be the AoI at time step t for node x, where $\Delta_i[t]$, $\Delta_j[t]$, $\Delta_b[t]$, and $\Delta_{\text{CS}}[t]$, denote the AoI for the i-th SBS, j-th MBS, b-th wired backhaul link, and the cloud server, respectively. Then, $\Delta_x[t]$ is modeled as [9]:

$$\Delta_x[t] = \begin{cases} 0, & \text{if } \psi_x[t] = 1, x \in \{i, j\} \\ \Delta_j[t], & \text{if } \psi_b[t] = 1, b = 1 \\ \Delta_{b-1}[t], & \text{if } \psi_b[t] = 1, 2 \leq b \leq N-1 \\ \Delta_{N-1}[t], & \text{if } \psi_{\text{CS}}[t] = 1 \\ \Delta_x[t-1] + 1, & \text{if } \psi_x[t] = 0, x \in \{i, j, b, \text{CS}\} \end{cases} \tag{2}$$

where $\psi_x[t] = 1$ denotes successful packet reception with time invariant probability $1 - p_{\text{x}}$ [9], and $\psi_x[t] = 0$ denotes packet reception failure with probability p_{x}.

[1] An example of this will be real-time video analytics, where each video frame is considered a task and is transmitted as a single packet for computation.

[2] With multiple tasks, each task is sequentially transmitted as a packet over a transmission timeslot, with older packets at the AMR discarded regardless of successful transmissions due to limited buffer space [9].

[3] Future works can investigated the impact of computation offloading as a source of co-channel interference in IIoT networks.

[4] Similar assumptions have been adopted in [10] for vehicular networks, where vehicles operate in a similar fashion to AMRs.

[5] It is worth emphasizing that block fading is assumed in this work for cellular and wired backhaul links.

[6] The spatial locations of the SBSs, MBSs, and IAMRs, are modeled as binomial point processes in this work.

[7] The AoI in the MEC-enabled IIoT network increases linearly when discrete time steps are adopted, as depicted in [9, Fig. 2].

III. Age of Information Outage Probability Analysis

In this section, closed-form AoI outage probability expression are presented for MEC-CO in the MEC-enabled IIoT network. As a benchmark, the closed-form AoI outage probability for CLD-CO in the MEC-enabled IIoT network is also presented.

In MEC-CO, tasks from the AMR are offloaded either to the i-th SBS or to the cloud server via the j-th MBS. The former occurs when the AoI of the i-th SBS is in outage. As such, based on [17, eq. (5)], the AoI outage probability for the x-th node is defined as $\mathbb{P}\{\Delta_x[t] \geq \delta_x\}$, where $\delta_x \geq 0$ indicates the number of unsuccessful retransmissions in order for an outage to be declared, i.e., probability that the AoI violates δ_x. Then, the AoI outage probability for MEC-CO is defined as $\mathbb{P}\{O_{\text{MEC-CO}}\} = \mathbb{P}\{\Delta_i[t] \geq \delta_i\}\mathbb{P}\{\Delta_{\text{CS}}[t] \geq \delta_{N-1}\}$

It is noted that obtaining $\mathbb{P}\{O_{\text{MEC-CO}}\}$ in closed-form necessitates that one obtains the AoI occurrence probability ($\mathbb{P}\{\Delta_n[t] = \delta_n\}$) for nodes located $2 \leq n \leq N$ hops from the AMR. To this end, the closed-form expression of $\mathbb{P}\{\Delta_n[t] = \delta_n\}$ is presented in the following lemma which can be computed recursively using [9, Algorithm 1] or via iterative means.

Lemma 1: The closed-form expression for the AoI occurrence probability of a node located $2 \leq n \leq N$ hops from the AMR is:

$$\mathbb{P}\{\Delta_n[t] = \delta_n\} = \left[\prod_{q=1}^{n}(1-p_q)\right] \sum_{\substack{\delta_1,\ldots,\delta_n \\ 0\leq\delta_1\leq\delta_w\leq\ldots\leq\delta_n}} p_1^{\delta_1} \prod_{w=2}^{n} p_w^{\delta_w-\delta_{w-1}}. \quad (3)$$

Proof: The proof is given in Appendix A. ∎

For nodes with direct transmissions, i.e., next hop, from the AMR, the AoI occurrence probability $\mathbb{P}\{\Delta_1[t] = \delta_1\}$ can be obtained via [9, eq. (2)]. However, before one can apply (3) and [9, eq. (2)] to obtain the closed-form expression of $\mathbb{P}\{O_{\text{MEC-CO}}\}$, the closed-form CDF expressions of γ_i ($F_{\gamma_i}(\gamma_{\text{tx}})$) and γ_j ($F_{\gamma_j}(\gamma_{\text{tx}})$), i.e., outage probability of $\gamma_x, x \in \{i, j\}$, must also be obtained.

Let $\gamma_{\text{tx}} = 2^{\frac{K_{\text{size}}}{\tau B W}} - 1$ be the SINR threshold, and τ be the time-out threshold in seconds. Then, the closed-form expression of $F_{\gamma_x}(\gamma_{\text{tx}}), x \in \{i, j\}$ is presented in the following lemma:

Lemma 2: The closed-form expression for $F_{\gamma_x}(\gamma_{\text{tx}})$ is:

$$F_{\gamma_x}(\gamma_{\text{tx}}) = (1-\mathbb{P}_{\text{LOS}}) + \mathbb{P}_{\text{LOS}} \sum_{p=0}^{K_{\text{tr}}} \sum_{c_1+\ldots+c_{M_{\text{int}}+2}=p+1} \alpha_x(p) \times \binom{c_1+\ldots+c_{M_{\text{int}}+2}}{c_1,\ldots,c_{M_{\text{int}}+2}} \Xi_x(p, c_{M_{\text{int}}+1}) \left[\prod_{z=1}^{M_{\text{int}}} \Theta_z(c_z)\right], \quad (4)$$

where $x \in \{i, j\}$, K_{tr} is the truncation order, $\alpha_x(p) = \frac{(-1)^p \exp(-K_x) L_p^{(0)}(K_x[\gamma_{\text{tx}}(1+K_x)]^{p+1}}{(p+1)!(\Omega_x)^{p+1}}$ is the CDF expansion of γ_x, $\Xi_x(p, c_{M_{\text{int}}+1}) = \frac{2(r_{\text{a}})^{l(p+1-c_{M_{\text{int}}+1})}}{l(p+1-c_{M_{\text{int}}+1})+2}(\mu_x)^{c_{M_{\text{int}}+1}}\Gamma(c_{M_{\text{int}}+1}+1)$ is the $c_{M_{\text{int}}+1}$-th moment of $|e_x|^2 d_x^{-l}$, $\Theta_z(c_z) = \frac{\Gamma(c_z+1)(\Omega_z)^{c_z}}{(1+K_z)^{c_z}} {}_1F_1(-c_z, 1; -K_z) \frac{2\left[(r_{\text{int}})^{2-l\cdot c_z} - (r_{\text{a}})^{2-l\cdot c_z}\right]}{[r_{\text{int}}^2 - r_{\text{a}}^2][2-l\cdot c_z]}$ is the c_z-th moment of $|h_z|^2 d_z^{-l}$, $\Gamma(\bullet)$ is the Gamma function, ${L_p}^{(0)}(\bullet)$ is the p-th degree, zero-order Laguerre polynomials [11], and ${}_1F_1(\bullet)$ is the confluent Hypergeometric function [11].

Proof: The proof is given in Appendix B. ∎

From Lemma 1 and Lemma 2, the closed-form expression for $\mathbb{P}\{O_{\text{MEC-CO}}\}$ is presented in the following theorem:

Theorem 1: The closed-form expression for $\mathbb{P}\{O_{\text{MEC-CO}}\}$ is:

$$\mathbb{P}\{O_{\text{MEC-CO}}\} = \left(1 - \sum_{\delta_i=0}^{\varpi_i} \hat{\alpha}_i(\delta_i)\right) \times \left(1 - \sum_{\delta_{N-1}=0}^{\varpi_{\text{CS}}} \sum_{\substack{\delta_j,\delta_1,\ldots,\delta_{N-1} \\ 0\leq\delta_j\leq\delta_1\leq\ldots\leq\delta_{N-1}}} \hat{\alpha}_{\text{CS}}(\delta_{N-1})\right), \quad (5)$$

where $\hat{\alpha}_i(\delta_i) = \left[1 - \left(F_{\gamma_i}(\gamma_{\text{tx}})\right)^{M_{\text{SBS}}}\right]\left[F_{\gamma_i}(\gamma_{\text{tx}})\right]^{M_{\text{SBS}}\delta_i}$, $\hat{\alpha}_{\text{CS}}(\delta_{N-1}) = \left[1 - \left(F_{\gamma_j}(\gamma_{\text{tx}})\right)^{M_{\text{MBS}}}\right]\left[F_{T_b}(\tau_{\text{BH}})\right]^{N-1} \times \left[F_{\gamma_j}(\gamma_{\text{tx}})\right]^{M_{\text{MBS}}\delta_j}\left(1 - F_{T_b}(\tau_{\text{BH}})\right)^{\delta_1-\delta_j+\sum_{b=2}^{N-1}\delta_b-\delta_{b-1}}$, $F_{T_b}(\tau_{\text{BH}}) = \frac{\Gamma\left(m_\omega, \frac{\tau_{\text{BH}}}{\theta_\omega}\right)}{\Gamma(m_\omega)}$ is the CDF of T_b [18, Table II], τ_{BH} is the wired backhaul timeout threshold, $F_{\gamma_x}(\gamma_{\text{tx}}), x \in \{i, j\}$ is obtained using (4), ϖ_i is the AoI outage threshold at the i-th SBS, ϖ_{CS} is the AoI outage threshold at the cloud server, and $\Gamma(\bullet, \bullet)$ is the incomplete Gamma function.

Proof: The proof is given in Appendix C. ∎

For CLD-CO, the AoI outage probability $\mathbb{P}\{O_{\text{CLD-CO}}\}$ in the MEC-enabled IIoT network is defined as $\mathbb{P}\{O_{\text{CLD-CO}}\} = \mathbb{P}\{\Delta_{\text{CS}}[t] \geq \delta_{N-1}\}$. Then, the closed-form expression for $\mathbb{P}\{O_{\text{CLD-CO}}\}$ is presented in the following theorem:

Theorem 2: The closed-form expression for $\mathbb{P}\{O_{\text{CLD-CO}}\}$ is:

$$\mathbb{P}\{O_{\text{CLD-CO}}\} = \left(1 - \sum_{\delta_{N-1}=0}^{\varpi_{\text{CS}}} \sum_{\substack{\delta_j,\delta_1,\ldots,\delta_{N-1} \\ 0\leq\delta_j\leq\delta_1\leq\ldots\leq\delta_{N-1}}} \hat{\alpha}_{\text{CS}}(\delta_{N-1})\right). \quad (6)$$

Proof: The closed-form expression in (6) is obtained using the same approach in Appendix C. ∎

The closed-form expressions in (5) and (6) enable the analysis of AoI outage probability while realistically modeling the deployment of nodes in IIoT scenarios, with a complexity of $O(\varpi_{\text{CS}}\delta_j\prod_{b=2}^{N-1}\delta_b)$. [8] Specifically, larger values of K_{size} and r_{a}, and a smaller $\mathbb{P}_{\text{LOS}}$, increases AoI outage probability. Furthermore, (5) and (6) shows that the inclusion of the i-th SBS equipped with an MEC server contributes greatly to lower AoI outage probability in the MEC-enabled IIoT network.

IV. Numerical Results

In this section, numerical results are presented for the MEC-CO and CLD-CO protocols in the MEC-enabled IIoT network. Monte Carlo simulations are also conducted with 10^4 samples using the default simulation parameters in Table I with 95% confidence interval. [9] For the AoI outage probability analysis, the UMi and RMa scenarios from [19] are considered in this

[8] Future extensions of this work can investigate deep learning-based methods to predict AoI outage probability in order to reduce the computation time.

[9] Confidence interval is computed as $\bar{x} \pm t_x \frac{x_\sigma}{\sqrt{x_{\text{num}}}}$, where $\bar{x}$, x_σ, and x_{num}, respectively denote the mean, standard deviation, and total number of Monte Carlo samples and $t_x = 1.645$ is the critical t-value for 95% confidence interval.

TABLE I
DEFAULT SIMULATION PARAMETERS

Description	Value(s)
Cellular Transmissions	$K_{\text{size}} = 1$ MB, $f_c = 5.2$ GHz [20] $M_{\text{SBS}} = 3$, $M_{\text{MBS}} = 2$, $M_{\text{int}} = 2$ interferers $P_t = 44$ dBm [19], $\overline{P}_t = 74.7$ dB, $l = 2.59$ [20] $L_0 = 70.28$ dB [20], $B_w = 20$ MHz [19] $T = 0.5$ms [21], $v = 30$ km/h $\tau = 1.5$s, $\tau_{\text{BH}} = 15$s, $\varpi_i = 1$, $\varpi_{\text{CS}} = 2$ $r_a = d_b = 200$m, $r_{\text{int}} = 500$m $K_t = K_j = K_z = 5$ dB [4], $K_{\text{tr}} = 10$
LOS Probability Model	$\mathbb{P}_{\text{LOS}}^{\text{UMi}} = \frac{18}{r_a} + \left[1 - \frac{18}{r_a}\right] \exp(-r_a/36)$ [19] $\mathbb{P}_{\text{LOS}}^{\text{RMa}} = \exp\left(-\frac{r_a - 10}{1000}\right)$ [19]
Wired Backhaul Links	$N = 3$ hops, $c_{\text{wired}} = 10^{-8}$s [16]

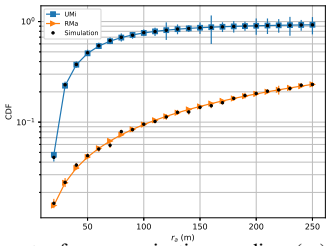

Fig. 2. The impact of communications radius (r_a) on the CDF of γ_x ($F_{\gamma_x}(\gamma_{\text{tx}})$) for $x \in \{i, j\}$.

paper. Correspondingly, $\mathbb{P}_{\text{LOS}} \in \left\{\mathbb{P}_{\text{LOS}}^{\text{UMi}}, \mathbb{P}_{\text{LOS}}^{\text{RMa}}\right\}$ where $\mathbb{P}_{\text{LOS}}^{\text{UMi}}$ and $\mathbb{P}_{\text{LOS}}^{\text{RMa}}$ are the LOS probability for the UMi and RMa scenarios, respectively.

The impact of communications radius (r_a) on the CDF of γ_x ($F_{\gamma_x}(\gamma_{\text{tx}})$), i.e., γ_x outage probability, for $x \in \{i, j\}$ is shown in Fig. 2 for the UMi and RMa scenarios. It is evident that the simulations are matching closely with the numerical results, thus validating the closed-form CDF expression in (4) for SINR $\gamma_x, x \in \{i, j\}$. It is further observed that the outage probability of γ_x is lower in the RMa scenario, due to the fact that $\mathbb{P}_{\text{LOS}}^{\text{RMa}} > \mathbb{P}_{\text{LOS}}^{\text{UMi}}$.

The impact of the cloud server's AoI outage threshold (ϖ_{CS}), task size (K_{size}), and communications radius (r_a), on AoI outage probability is shown in Fig. 3, Fig. 4, and Fig. 5, respectively. It is seen in Fig. 3, Fig. 4, and Fig. 5, that the AoI outage probability of the MEC-CO protocol ($\mathbb{P}\{O_{\text{MEC-CO}}\}$) is lower than the AoI outage probability of the CLD-CO protocol ($\mathbb{P}\{O_{\text{CLD-CO}}\}$) for both UMi and RMa scenarios. This is due to $\mathbb{P}_{\text{LOS}}^{\text{RMa}} > \mathbb{P}_{\text{LOS}}^{\text{UMi}}$, which leads to a lower outage probability for the SINR of the i-th SBS, i.e.,γ_i, in the MEC-enabled IIoT network. It is further noted in Fig. 3, that $\mathbb{P}\{O_{\text{MEC-CO}}\}$

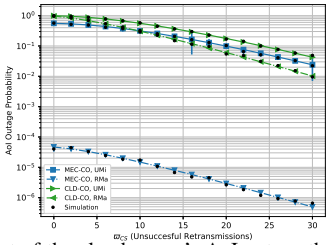

Fig. 3. The impact of the cloud server's AoI outage threshold (ϖ_{CS}) on AoI outage probability in the MEC-enabled IIoT network.

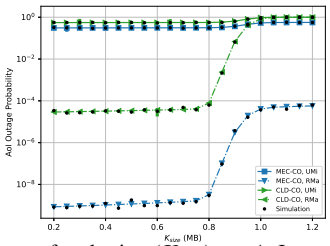

Fig. 4. The impact of task size (K_{size}) on AoI outage probability in the MEC-enabled IIoT network.

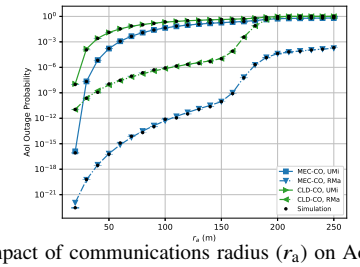

Fig. 5. The impact of communications radius (r_a) on AoI outage probability in the MEC-enabled IIoT network.

in the UMi scenario is higher than $\mathbb{P}\{O_{\text{CLD-CO}}\}$ in the RMa scenario when $\varpi_{\text{CS}} > 10$. In Fig. 4, it is observed that $\mathbb{P}\{O_{\text{CLD-CO}}\}$ is the same for both UMI and RMa scenarios when $K_{\text{size}} > 1$ MB. In contrast, $\mathbb{P}\{O_{\text{MEC-CO}}\}$ is the lowest for 0.2 MB $\leq K_{\text{size}} \leq 1.2$ MB in the RMa scenario. For Fig. 5, $\mathbb{P}\{O_{\text{MEC-CO}}\}$ and $\mathbb{P}\{O_{\text{CLD-CO}}\}$ are observed to be low when $r_a \leq 50$m in the UMi scenario. However, as $r_a > 50$m, both MEC-CO and CLD-CO attains similar AoI outage probability. In contrast, $\mathbb{P}\{O_{\text{MEC-CO}}\} < \mathbb{P}\{O_{\text{CLD-CO}}\}$ is observed in the RMa scenario for 20m $\leq r_a \leq$ 250m.

The above trends demonstrate that the MEC-CO protocol attains higher reliability than the CLD-CO protocol in both UMi and RMa scenarios. Furthermore, the AoI outage probability analysis shows that enabling reliable MEC-CO and CLD-CO in the UMi scenario necessitates r_a and K_{size} to be small. As a result, MEC-CO and CLD-CO in the UMi scenario may be more suitable for IIoT use cases employing short-packet communications. [10] In contrast, reliable computation offloading in the RMa scenario can be achieved with the MEC-CO protocol for large and small values of r_a and K_{size}.

V. CONCLUSION

The AoI outage probability of MEC-CO and CLD-CO is investigated in this paper for MEC-enabled IIoT networks. Using new CDF expressions of received SINRs, closed-form AoI outage probability expressions are obtained for a comprehensive performance analysis of both MEC-CO and CLD-CO protocols. Numerical and simulation results are used to identify communication radius and task size parameters to attain reliable computation offloading in MEC-enabled IIoT networks for both MEC-CO and CLD-CO. Extensive analysis under UMi and RMa scenarios also show the MEC-CO protocol attaining lower AoI outage probability, thus demonstrating it's viability towards enabling mission-critical IIoT use cases.

APPENDIX A
PROOF OF LEMMA 1

From [9, eq. (5)], the AoI occurrence probability for $n = 2$ hops from the AMR, i.e., $\mathbb{P}\{\Delta_2[t] = \delta_2\}$, is $\mathbb{P}\{\Delta_2[t] = \delta_2\} = (1 - p_1)(1 - p_2) \sum_{\delta_1=0}^{\delta_2} p_2^{\delta_2 - \delta_1} p_1^{\delta_1}$. Likewise, the AoI occurrence probability for $n = 3$ hops from the AMR, i.e., $\mathbb{P}\{\Delta_3[t] = \delta_3\}$, is $\mathbb{P}\{\Delta_3[t] = \delta_3\} = \left[\prod_{q=1}^{3}(1 - p_q)\right] \sum_{\delta_2=0}^{\delta_3} \sum_{\delta_1=0}^{\delta_2} p_1^{\delta_1} p_2^{\delta_2 - \delta_1} p_3^{\delta_3 - \delta_2}$ [9, eq. (9)]. Therefore, for $n \geq 2$ hops from the AMR, the occurrence probability, i.e., $\mathbb{P}\{\Delta_n[t] = \delta_n\}$, is evaluated as $\mathbb{P}\{\Delta_n[t] = \delta_n\} = \left[\prod_{q=1}^{n}(1 - p_q)\right] \sum_{\delta_{n-1}=0}^{\delta_n} \cdots \sum_{\delta_1=0}^{\delta_2} p_1^{\delta_1} p_2^{\delta_2 - \delta_1} \cdots p_n^{\delta_n - \delta_{n-1}}$ [9,

[10] Characterizing the AoI outage probability of short-packet communications in IIoT networks is left as a future extension of this work.

eq. (9)]. Finally, applying algebraic simplifications yields the closed-form expression in (3), which completes the proof.

Appendix B
Proof of Lemma 2

We begin by noting that the CDF of $\gamma_x, x \in \{i, j\}$ conditioned on d_x, d_z, $|e_x|^2$, and $|h_z|^2$, i.e., $F_{\gamma_x|d_x,d_z,|e_x|^2,|h_z|^2}(\gamma_{\text{tx}})$, can be expressed as follows using the power series approach [11, Lemma 1]:

$$\begin{aligned} F_{\gamma_x|d_x,d_z,|e_x|^2,|h_z|^2}(\gamma_{\text{tx}}) &= (1-\mathbb{P}_{\text{LOS}}) \\ &+\mathbb{P}_{\text{LOS}} \sum_{p=0}^{K_{\text{tr}}} \frac{(-1)^p \exp(-K_x) L_p^{(0)}(K_x)[\gamma_{\text{tx}}(1+K_x)]^{p+1}}{(p+1)!(\Omega_x)^{p+1}} \\ &\times \sum_{c_1+\ldots+c_{M_{\text{int}}+2}=p+1} \binom{c_1+\ldots+c_{M_{\text{int}}+2}}{c_1,\ldots,c_{M_{\text{int}}+2}} (d_x)^{l(p+1-c_{M_{\text{int}}+1})} \\ &\times \left(|e_x|^2\right)^{c_{M_{\text{int}}+1}} \prod_{z=1}^{M_{\text{int}}} \left(|h_z|^2 d_z^{-l}\right)^{c_z}, \end{aligned} \tag{7}$$

where the first term in (7) is due outage caused by LOS blockage. Thereafter, applying [11, Lemma 1] and [18, Table II] to average (7) with respect to d_x, d_z, $|e_x|^2$, and $|h_z|^2$ yields (4). This completes the proof.

Appendix C
Proof of Theorem 1

It is noted that $\mathbb{P}\{O_{\text{MEC-CO}}\}$ can be rewritten as:

$$\begin{aligned} \mathbb{P}\{O_{\text{MEC-CO}}\} &= \left[1 - \sum_{\delta_i=0}^{\varpi_i} \mathbb{P}\{\Delta_i[t] = \delta_i\}\right] \\ &\times \left[1 - \sum_{\delta_{N-1}=0}^{\varpi_{\text{CS}}} \mathbb{P}\{\Delta_{\text{CS}}[t] = \delta_{N-1}\}\right]. \end{aligned} \tag{8}$$

Starting with the i-th SBS and j-th MBS, let $\phi_i = \frac{K_{\text{size}}}{B_W \log_2(1+\max_{1\le i\le M_{\text{SBS}}}(\gamma_i))}$ and $\phi_j = \frac{K_{\text{size}}}{B_W \log_2(1+\max_{1\le j\le M_{\text{MBS}}}(\gamma_j))}$ be the respective task transmission latencies. Then, the Aoi occurrence probability $\mathbb{P}\{\Delta_x[t] = \delta_x\}, x \in \{i, j\}$ for the i-th SBS and j-th MBS can be obtained as [9, eq. (2)]:

$$\begin{aligned} \mathbb{P}\{\Delta_x[t] = \delta_x\} &= (1-p_x)(p_x)^{\delta_x} \\ &\overset{(a)}{=} \left[1 - \left(F_{\gamma_x}(\gamma_{\text{tx}})\right)^{M_x}\right] \left[F_{\gamma_x}(\gamma_{\text{tx}})\right]^{M_x \delta_x}, \end{aligned} \tag{9}$$

where $M_x = M_{\text{SBS}}$ for $x = i$, $M_x = M_{\text{MBS}}$ for $x = j$, $p_x = \left(\mathbb{P}\{\gamma_x \le \gamma_{\text{tx}}\}\right)^{M_x}$, and (a) is obtained using Lemma 2.

For the cloud server, the AoI occurrence probability $\mathbb{P}\{\Delta_{\text{CS}}[t] = \delta_{N-1}\}$ is obtained from Lemma 1 as:

$$\begin{aligned} \mathbb{P}\{\Delta_{\text{CS}}[t] = \delta_{N-1}\} &= \left[1 - \left(F_{\gamma_j}(\gamma_{\text{tx}})\right)^{M_{\text{MBS}}}\right] \left[F_{T_b}(\tau_{\text{BH}})\right]^{N-1} \\ &\times \sum_{\substack{\delta_j, \delta_1, \ldots, \delta_{N-1} \\ 0 \le \delta_j \le \delta_1 \le \ldots \le \delta_{N-1}}} \left[F_{\gamma_j}(\gamma_{\text{tx}})\right]^{M_{\text{MBS}} \delta_j} \\ &\times \left(1 - F_{T_b}(\tau_{\text{BH}})\right)^{\delta_1 - \delta_j + \sum_{b=2}^{N-1} \delta_b - \delta_{b-1}}, \end{aligned} \tag{10}$$

where $p_b = \mathbb{P}\{T_b > \tau_{\text{BH}}\} = 1 - \frac{\Gamma\left(m_\omega, \frac{\tau_{\text{BH}}}{\theta_\omega}\right)}{\Gamma(m_\omega)} = 1 - F_{T_b}(\tau_{\text{BH}})$. Thereafter, substituting (9) and (10) into (8) yields the closed-form expression in (5). This completed the proof.

References

[1] Z. Zhao, R. Zhao, J. Xia, X. Lei, D. Li, C. Yuen, and L. Fan, "A novel framework of three-hierarchical offloading optimization for MEC in industrial IoT networks," *IEEE Trans. Ind. Informat.*, vol. 16, no. 8, pp. 5424–5434, 2019.

[2] M. Khoshnevisan, V. Joseph, P. Gupta, F. Meshkati, R. Prakash, and P. Tinnakornsrisuphap, "5G industrial networks with CoMP for URLLC and time sensitive network architecture," *IEEE J. Sel. Areas Commun.*, vol. 37, no. 4, pp. 947–959, April 2019.

[3] T. Jiang, J. Zhang, P. Tang, L. Tian, Y. Zheng, J. Dou, H. Asplund, L. Raschkowski, R. D'Errico, and T. Jämsä, "3GPP Standardized 5G Channel Model for IIoT Scenarios: A Survey," *IEEE Internet Things J.*, vol. 8, no. 11, pp. 8799–8815, 2021.

[4] M. Eriksson and T. Olofsson, "On long-term statistical dependences in channel gains for fixed wireless links in factories," *IEEE Trans. Commun.*, vol. 64, no. 7, pp. 3078–3091, July 2016.

[5] D. Van Huynh, V.-D. Nguyen, S. Chatzinotas, S. R. Khosravirad, H. V. Poor, and T. Q. Duong, "Joint Communication and Computation Offloading for Ultra-Reliable and Low-Latency with Multi-tier Computing," *IEEE J. Sel. Areas Commun.*, February 2023.

[6] S. Bebortta, D. Senapati, C. R. Panigrahi, and B. Pati, "An adaptive performance modeling framework for QoS-aware offloading in MEC-based IIoT systems," *IEEE Internet Things J.*, June 2022.

[7] H. Hu, J. Zhang, Y. Jiang, Z. Li, Q. Chen, and J. Zhang, "Computation Offloading Analysis in Clustered Fog Radio Access Networks With Repulsion," *IEEE Trans. Veh. Technol.*, vol. 70, no. 10, pp. 10 804–10 819, 2021.

[8] A. Hazra and T. Amgoth, "CeCO: Cost-efficient computation offloading of IoT applications in green industrial fog networks," *IEEE Trans. Ind. Informat.*, September 2022.

[9] O. Ayan, H. M. Gürsu, A. Papa, and W. Kellerer, "Probability analysis of age of information in multi-hop networks," *IEEE Netw. Lett.*, vol. 2, no. 2, pp. 76–80, June 2020.

[10] T. Z. H. Ernest and A. S. Madhukumar, "Ensemble Learning-Based Edge Caching Strategies for Internet-of-Vehicles: Outage and Finite SNR Analysis," *IEEE Open J. Commun. Soc.*, 2023.

[11] T. Z. H. Ernest, A. S. Madhukumar, R. P. Sirigina, and A. K. Krishna, "Hybrid-Duplex Communications for Multi-UAV Networks: An Outage Probability Analysis," *IEEE Commun. Lett.*, vol. 23, no. 10, pp. 1831–1835, October 2019.

[12] M. Derakhshani and T. Le-Ngoc, "Aggregate Interference and Capacity-Outage Analysis in a Cognitive Radio Network," *IEEE Trans. Veh. Technol.*, vol. 61, no. 1, pp. 196–207, Jan. 2012.

[13] M. Abramowitz and I. Stegun, "Handbook of mathematical functions with formulas, graphs, and mathematical tables (applied mathematics series 55)," *National Bureau of Standards, Washington, DC*, 1964.

[14] B. Maham and P. Popovski, "Capacity Analysis of Coordinated Multi-point Reception for mmWave Uplink with Blockages," *IEEE Trans. Veh. Technol.*, December 2020.

[15] A. E. Kalør, O. Simeone, and P. Popovski, "Prediction of mmWave/THz link blockages through meta-learning and recurrent neural networks," *IEEE Wireless Commun. Lett.*, vol. 10, no. 12, pp. 2815–2819, 2021.

[16] J. Park, P. Popovski, and O. Simeone, "Minimizing latency to support VR social interactions over wireless cellular systems via bandwidth allocation," *IEEE Wireless Commun. Lett.*, vol. 7, no. 5, pp. 776–779, October 2018.

[17] W. He, C. Guo, and X. Wang, "Age of Information Aware Resource Allocation and Packet Sampling Control in Vehicular Networks," *IEEE Wireless Commun. Lett.*, vol. 11, no. 11, pp. 2245–2249, 2022.

[18] N. B. Rached, A. Kammoun, M.-S. Alouini, and R. Tempone, "A unified moment-based approach for the evaluation of the outage probability with noise and interference," *IEEE Trans. Wireless Commun.*, vol. 16, no. 2, pp. 1012–1023, 2017.

[19] ETSI, "Study on channel model for frequencies from 0.5 to 100 GHz (3GPP TR 38.901 version 16.1.0 Release 16)," Tech. Rep., 2020.

[20] E. Tanghe, W. Joseph, L. Verloock, L. Martens, H. Capoen, K. Van Herwegen, and W. Vantomme, "The industrial indoor channel: large-scale and temporal fading at 900, 2400, and 5200 mhz," *IEEE Trans. Wireless Commun.*, vol. 7, no. 7, pp. 2740–2751, July 2008.

[21] X. Li, L. Ma, Y. Xu, and R. Shankaran, "Resource allocation for D2D-based V2X communication with imperfect CSI," *IEEE Internet Things J.*, vol. 7, no. 4, pp. 3545–3558, April 2020.